

## SONOCHEMICAL SYNTHESIS AND CHARACTERIZATION OF Mg-DOPED BiOI AS VISIBLE-LIGHT-DRIVEN PHOTOCATALYST

P. INTAPHONG<sup>a</sup>, A. PHURUANGRAT<sup>a,\*</sup>, N. EKTHAMMATHAT<sup>b</sup>,  
S. THONGTEM<sup>c,d</sup>, T. THONGTEM<sup>d,e</sup>

<sup>a</sup>*Department of Materials Science and Technology, Faculty of Science,  
Prince of Songkla University, Hat Yai, Songkhla 90112, Thailand*

<sup>b</sup>*Program of Chemistry, Faculty of Science and Technology,  
Bansomdejchaopraya Rajabhat University, Bangkok 10600, Thailand*

<sup>c</sup>*Department of Physics and Materials Science, Faculty of Science,  
Chiang Mai University, Chiang Mai 50200, Thailand*

<sup>d</sup>*Materials Science Research Center, Faculty of Science, Chiang Mai University,  
Chiang Mai 50200, Thailand*

<sup>e</sup>*Department of Chemistry, Faculty of Science, Chiang Mai University,  
Chiang Mai 50200, Thailand*

Mg-doped BiOI nanostructures as visible-light-driven photocatalyst were synthesized by a sonochemical method. The products were characterized by X-ray diffraction (XRD), transmission electron microscopy (TEM), selected area electron diffraction (SAED) and X-ray photoelectron spectroscopy (XPS). In this research, the products were specified as tetragonal BiOI nanoplates and Mg-doped BiOI nanobelts. Photocatalytic activities of the samples were investigated by degradation of rhodamine B (RhB) under visible light irradiation. The Mg-doped BiOI show significantly improved photocatalytic activity for the degradation of RhB under visible light irradiation as compared to pure BiOI sample. The mechanism of photodegradation of RhB by Mg-doped BiOI was discussed in this research.

(Received August 5, 2018; Accepted November 12, 2018)

*Keywords:* Mg-doped BiOI; Photocatalyst; Nanobelts; Sonochemical method

### 1. Introduction

Recently, bismuth oxyhalides BiOX (X = Br, Cl and I) have been found to be promising visible light photocatalysts due to their unique layered structure, high activity, high photocorrosion stability, and excellent electrical and optical properties [1, 2]. Among them, BiOI shows an excellent photocatalyst to decompose organic compounds into inorganic substances containing in polluted wastewater due to its low band gap energy (1.7–1.9 eV) and strong absorption in visible-light region [1, 3, 4]. Nevertheless, utilizing BiOI is disadvantage in photocatalytic application because of its rapid electron-hole pair recombination [1, 3]. Metal ion dopant may also be an effective way to improve the photocatalytic activity by improving charge separation of photogenerated electrons and holes [5, 6].

In the present research, Mg-doped BiOI photocatalysts were synthesized using an ultrasonic method. The products were characterized by X-ray diffraction (XRD), transmission electron microscopy (TEM), selected area electron diffraction (SAED) and X-ray photoelectron spectroscopy (XPS). The photocatalytic performance of as-prepared Mg-doped BiOI photocatalyst was evaluated for photocatalytic degradation of rhodamine B (RhB) as model dye under visible light illumination.

---

\*Corresponding author: phuruangrat@hotmail.com

## 2. Experimental procedure

To synthesize 0–10 wt% Mg-doped BiOI, 0.005 mole  $\text{Bi}(\text{NO}_3)_3 \cdot 6\text{H}_2\text{O}$  and NaI, and 0–10%  $\text{Mg}(\text{NO}_3)_2$  by weight were dissolved in 100 ml deionized water under vigorous stirring until complete dissolution. Subsequently, 3 M NaOH solution was slowly added to these solutions until reaching at the pH of 12. They were processed in 35 kHz ultrasonic bath at 80 °C for 5 h. The precipitates were collected, washed and dried for further characterization.

Photocatalysis was carried out as follows. 200 mg of catalyst was dispersed in 200 ml of  $1 \times 10^{-5}$  M RhB aqueous solutions. The suspensions were kept in the dark for 30 min under magnetical stirring before visible light illumination from a Xe lamp. At a given time interval, 5 ml sample was collected and centrifuged. The residual concentration of RhB was measured at 554 nm using a UV–visible spectrophotometer.

## 3. Results and discussion

Phase, structure and purity of as-synthesized pure BiOI and Mg-doped BiOI samples were investigated by XRD as the results shown in Fig. 1. All the diffraction peaks of pure BiOI and 1 wt% Mg-doped BiOI can be indexed to the tetragonal phase of BiOI in agreement to that of the JCPDS no. 10-0445 [7]. It can be seen that the diffraction angle of the (110) plane of doped sample was shift toward higher angle because ionic radius of  $\text{Mg}^{2+}$  (0.057 nm [6]) is smaller than that of  $\text{Bi}^{3+}$  (0.096 nm [8]). It confirmed the incorporation of  $\text{Mg}^{2+}$  ions in BiOI lattice. Moreover, the mixed phase of orthorhombic  $\text{Bi}_5\text{IO}_7$  structure (JCPDS no. 40-0548 [7]) as major phase and tetragonal BiOI structure as minor phase were detected by doping with Mg of > 1 % by weight. Therefore, the limit content of Mg doped in BiOI lattice is 1% by weight.

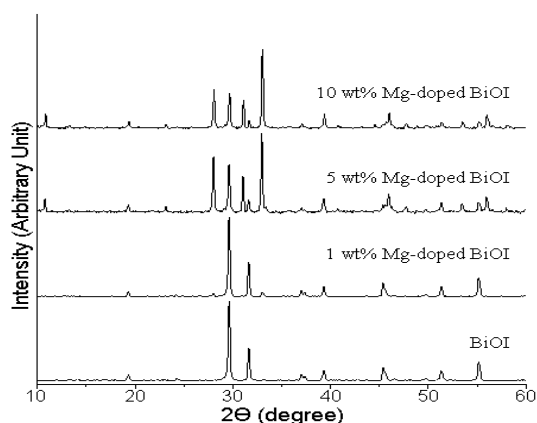


Fig. 1. XRD patterns of 0–10 wt% Mg-doped BiOI.

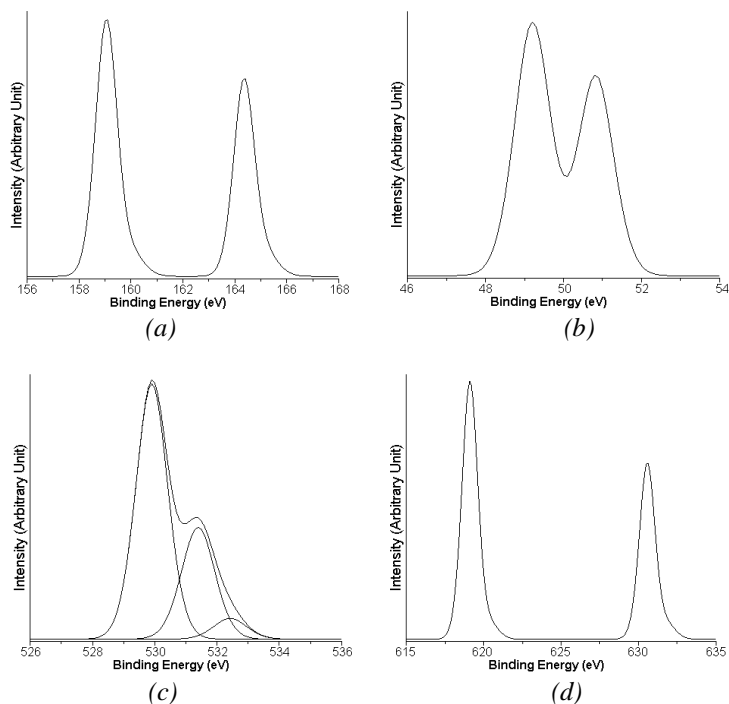


Fig. 2. XPS spectra of (a) Mg 2p and I 4d, (b) Bi 4f, (c) O 1s and (d) I 3d of 1 wt% Mg-doped BiOI synthesized by sonochemical method.

To further verify surface chemical composition of the sample, XPS spectra of as-prepared sample were carried out. Fig. 2a shows an overlap binding energies at 49.22 eV (Mg 2p<sub>3/2</sub>) and 50.8 eV (I 4d<sub>5/2</sub>), suggesting that Mg was doped in the BiOI crystal in the form of Mg<sup>2+</sup> [9–11]. The XPS spectrum (Fig. 2b) shows two peaks at binding energies of 159.06 eV and 164.35 eV which were assigned to Bi 4f<sub>7/2</sub> and Bi 4f<sub>5/2</sub> of Bi<sup>3+</sup> in the Mg-doped BiOI sample [12, 13]. The XPS spectrum of O 1s can be fitted to five peaks at 529.85, 531.20, 532.01, 533.07 and 534.20 eV demonstrating that there are five different kinds of oxygen species containing in the sample. The O 1 s peak (Fig. 2c) at 529.85, 531.20 and 532.01eV can be assigned to the Bi–O, Bi–O–Mg and Mg–O in Mg-doped BiOI sample [12, 13, 14]. Other XPS peaks of O 1s are the O–H bonds of adsorbed H<sub>2</sub>O and C–O bonds of adsorbed ambient atmosphere on the surface of BiOI [13, 15, 16]. The I 3d core level of Mg-doped BiOI (Fig. 2d) was detected at 619.12 and 630.62 eV corresponding to I 3d<sub>5/2</sub> and I 3d<sub>3/2</sub>, associating with I<sup>-</sup> ions in Mg-doped BiOI sample [12, 13]. According to the results, they confirmed that Mg ions have been successfully doped into the BiOI lattice.

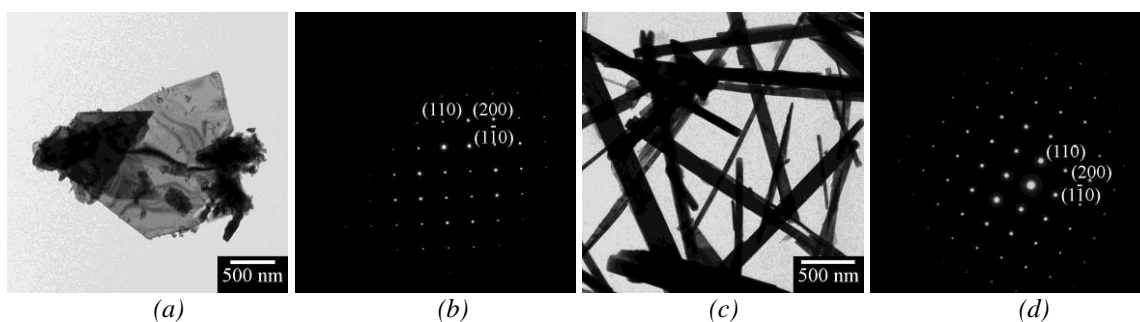


Fig. 3. TEM images and SAED patterns of (a, b) BiOI and (c, d) 1 wt% Mg-doped BiOI synthesized by sonochemical method.

Fig. 3 shows the TEM images and SAED patterns of BiOI and 1 wt% Mg-doped BiOI samples. The pure BiOI phase shows nanoplates with a diameter of 200–400 nm. Its SAED pattern was indexed to the (110), (200) and (1–10) planes of [00–1] direction for tetragonal BiOI structure which can be concluded that the bottom and top surfaces of BiOI nanoplate was the (001) facets. The morphology of product changed to nanobelts with aspect ratio of 50–70 for 1 wt% Mg-doped BiOI. The SAED pattern of Mg-doped BiOI nanobelts from a single nanobelt was indexed to the (110) (200) and (1–10) plane with zone axis of [00–1] which indicated that Mg-doped BiOI nanobelts are highly exposed (001) facets.

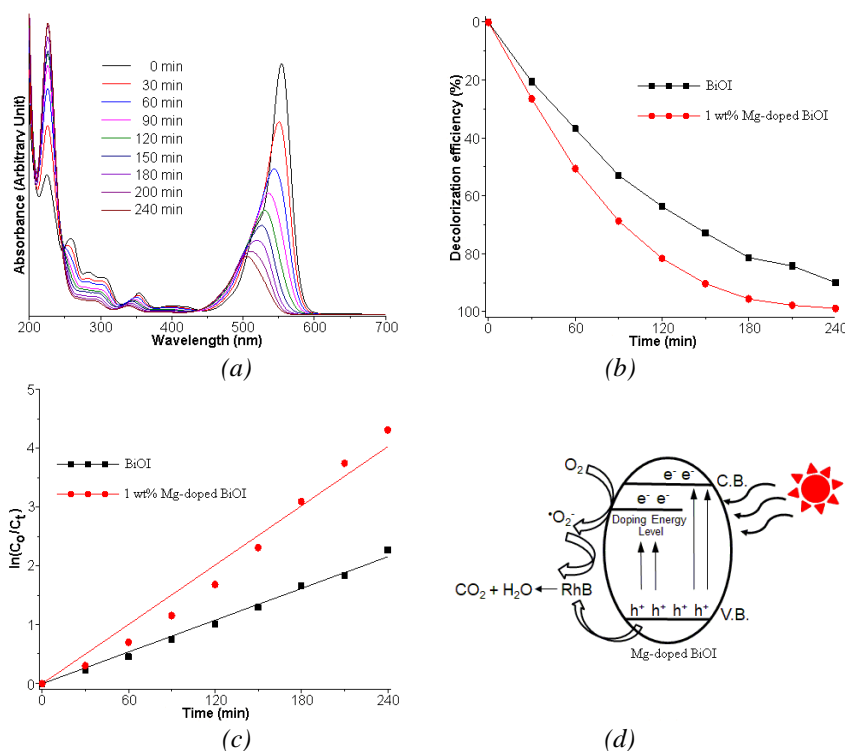


Fig. 4. (a) Absorbance of RhB solution photocatalyzed by 1 wt% Mg-doped BiOI. (b) Photocatalytic efficiency and (c)  $\ln(C_0/C_t)$  of BiOI and 1 wt% Mg-doped BiOI for different lengths of time under visible radiation. (d) Schematic illustration for photocatalytic mechanism of Mg-doped BiOI.

Fig. 4a shows the spectral change in the range of 200–700 nm for RhB during degradation reaction photocatalyzed by the 1 wt% Mg-doped BiOI. It was found that the absorption peak of RhB solution at 554 nm continuously decreased with the increase of irradiation time. It can be observed that the maximum absorption peak of RhB was blue shifted to 498 nm which was attributed to the de-ethylated reaction in the irradiating process [15, 16]. Fig. 4b shows the photocatalytic performance of RhB degradation using photocatalysts under visible light irradiation. It can be seen that 1 wt% Mg-doped BiOI as photocatalyst shows higher photocatalytic degradation of RhB under visible light irradiation than pure BiOI phase, which can be attributed to inhibit electron-hole recombination in photocatalytic reaction of BiOI. After 240 min of visible light irradiation, the performance of RhB degradation was 89.8% for pure BiOI and was 98.6% for 1 wt% Mg-doped BiOI. It can be concluded that the photocatalytic activity of BiOI was significantly improved by Mg dopant. The reaction kinetics of RhB degradation over photocatalyst was calculated by Eq (1).

$$\ln(C_0/C_t) = k_{app}t \quad (1)$$

, where  $C_0$ ,  $C_t$ ,  $k_{app}$  and  $t$  are the initial concentration, the concentration at different reaction time, the apparent reaction rate constant and the reaction time, respectively [15, 16]. Fig. 4c shows the plot between the  $\ln(C_0/C_t)$  and reaction time of RhB degradation over photocatalyst within 240

min. They show a well linear relationship indicating that the photocatalytic reaction belongs to a pseudo-first-order reaction. The apparent reaction rate constants for degradation performance of RhB by pure BiOI and 1 wt% Mg-doped BiOI were  $8.94 \times 10^{-3}$  and  $0.0167 \text{ min}^{-1}$ . The 1 wt% Mg-doped BiOI showed 1.87 times reaction rate constant of that of pure BiOI, indicating that photocatalytic activity of Mg-doped BiOI was enhanced.

Fig. 4d shows the schematic mechanism for photocatalytic reaction of RhB degradation by Mg-doped BiOI under visible light irradiation. After visible light irradiation, photogenerated electrons and holes were excited to valence band and conduction band of BiOI [1, 4, 12]. Subsequently, they diffused to surface of BiOI and reacted with  $\text{O}_2$  and  $\text{H}_2\text{O}$  molecules to form superoxide anion radical ( $\cdot\text{O}_2^-$ ) and hydroxyl radical ( $\cdot\text{OH}$ ) [1, 4]. In the end, RhB was degraded by these strong oxidants to  $\text{CO}_2$  and  $\text{H}_2\text{O}$  as final products [1, 4, 12]. When Mg ions were doped in BiOI lattice, Mg 3s state as Fermi level showed up under the conduction band which may provide a favorable channel for the photo-induced charge carrier diffusion and accelerating the diffusion of electrons to  $\text{O}_2$  molecules [5, 6]. Thus, the recombination of the photo-generated charged carriers was effectively suppressed and the carriers participated in the photocatalytic process, leading to the enhancement of photocatalytic efficiency.

#### 4. Conclusions

In summary, Mg-doped BiOI was successfully synthesized via a sonochemical method. The Mg-doped BiOI samples displayed significantly improved photodegradation activity in removing RhB under visible light irradiation because of the inhibited recombination of photo-generated electron-hole pairs.

#### Acknowledgements

This research was financially supported by Human Resource Development Project in the Science Achievement Scholarship of Thailand (SAST), Thailand.

#### References

- [1] R. Vinoth, S. G. Babu, R. Ramachandran, B. Neppolian, *Appl. Surf. Sci.* 418, 163 (2017).
- [2] J. Hu, S. Weng, Z. Zheng, Z. Pei, M. Huang, P. Liu, *J. Hazard. Mater.* 264, 293 (2014).
- [3] B. Li, H. Huang, Y. Guo, Y. Zhang, *Appl. Surf. Sci.* 353, 1179 (2015).
- [4] Y. Li, J. Wang, H. Yao, L. Dang, Z. Li, *J. Mole.. Catal. A.* 334, 116 (2011).
- [5] N. C. S. Selvam, S. Narayanan, L. J. Kennedy, J. J. Vijaya, *J. Environ. Sci.* 25, 2157 (2013).
- [6] Y. Wang, X. Zhao, L. Duan, F. Wang, H. Niu, W. Guo, A. Ali, *Mater. Sci. Semicond. Process.* 29, 372 (2015).
- [7] Powder Diffraction File, JCPDS-ICDD, 12 Campus Bld, Newtown Sq, PA 19073-3273, USA, 2001.
- [8] D. Liang, Z. Ge, H. Li, B. Zhang, F. Li, *J. Alloy. Compd.* 708, 169 (2017).
- [9] A. Agrawal, T. A. Dar, P. Sen, *J. Nano-Electron. Phys.* 5, 02025 (2013).
- [10] W. Zeng, X. Yang, M. Shang, X. Xu, W. Yang, H. Hou, *Ceram. Inter.* 42, 10021 (2016).
- [11] S. I. Levkovets, O. Y. Khyzhun, G. L. Myronchuk, P. M. Fochuk, M. Piasecki, I. V. Kityk, A. O. Fedorchuk, V. I. Levkovets, L. V. Piskach, O. V. Parasyuk, *J. Electron. Spectrosc. Relat. Phenom.* 218, 13 (2017).
- [12] Y. Long, Y. Wang, D. Zhang, P. Ju, Y. Sun, *J. Colloid Interf. Sci.* 481, 47 (2016).
- [13] X. Wang, F. Li, D. Li, R. Liu, S. Liu, *Mater. Sci. Eng. B* 193, 112 (2015).
- [14] S. Chen, X. D. Xie, S. Y. Cao, T. G. Liu, L. W. Lin, X. H. Chen, Q. C. Liu, J. C. Kuang, Y. Xiao, *Mater. Sci.-Poland* 33, 460 (2015).
- [15] S. Jonjana, A. Phuruangrat, S. Thongtem, T. Thongtem, *Mater Lett.* 179, 162 (2016).
- [16] S. Jonjana, A. Phuruangrat, S. Thongtem, T. Thongtem, *Mater. Lett.* 175, 75 (2016).